



HAL
open science

Mobilization and preferential transport of soil particles during infiltration: A core-scale modeling approach

Samer Majdalani, Eric Michel, Liliana Di Pietro, Rafaël Angulo-Jaramillo,
Marine Rousseau

► To cite this version:

Samer Majdalani, Eric Michel, Liliana Di Pietro, Rafaël Angulo-Jaramillo, Marine Rousseau. Mobilization and preferential transport of soil particles during infiltration: A core-scale modeling approach. *Water Resources Research*, 2007, 43 (5), pp.W05401. 10.1029/2006WR005057 . insu-00386980

HAL Id: insu-00386980

<https://insu.hal.science/insu-00386980>

Submitted on 10 Mar 2021

HAL is a multi-disciplinary open access archive for the deposit and dissemination of scientific research documents, whether they are published or not. The documents may come from teaching and research institutions in France or abroad, or from public or private research centers.

L'archive ouverte pluridisciplinaire **HAL**, est destinée au dépôt et à la diffusion de documents scientifiques de niveau recherche, publiés ou non, émanant des établissements d'enseignement et de recherche français ou étrangers, des laboratoires publics ou privés.

Mobilization and preferential transport of soil particles during infiltration: A core-scale modeling approach

Samer Majdalani,¹ Eric Michel,² Liliana Di Pietro,² Rafael Angulo-Jaramillo,^{1,3} and Marine Rousseau¹

Received 23 March 2006; revised 10 January 2007; accepted 19 January 2007; published 1 May 2007.

[1] Understanding particle movement in soils is a major concern for both geotechnics and soil physics with regard to environmental protection and water resources management. This paper describes a model for mobilization and preferential transport of soil particles through structured soils. The approach combines a kinematic-dispersive wave model for preferential water flow with a convective-dispersive equation subject to a source/sink term for particle transport and mobilization. Particle detachment from macropore walls is considered during both the steady and transient water flow regimes. It is assumed to follow first-order kinetics with a varying detachment efficiency, which depends on the history of the detachment process. Estimates of model parameters are obtained by comparing simulations with experimental particle breakthrough curves obtained during infiltrations through undisturbed soil columns. Both water flux and particle concentrations are satisfactorily simulated by the model. Particle mobilization parameters favoring both attachment and detachment of particles are related to the incoming solution ionic strength by a Fermi-type function.

Citation: Majdalani, S., E. Michel, L. Di Pietro, R. Angulo-Jaramillo, and M. Rousseau (2007), Mobilization and preferential transport of soil particles during infiltration: A core-scale modeling approach, *Water Resour. Res.*, 43, W05401, doi:10.1029/2006WR005057.

1. Introduction

[2] Biotic and abiotic soil colloids have been known for almost two decades to facilitate the transport of adsorbed contaminants through the vadose zone [McCarthy and Zachara, 1989]. Such particles migrating in the soil matrix can be filtrated by small pores, but preferential flow in soil macropores (e.g., invertebrate burrows) leads to rapid breakthrough of the colloids [Jacobsen *et al.*, 1997; Laegdsmand *et al.*, 1999; McKay *et al.*, 2000; Rousseau *et al.*, 2004a]. Quantification of particle transport through macroporous soils is thus essential for an accurate estimation of the potential risks of contaminant leaching into groundwater.

[3] Particle transport in both homogeneous and natural soils is usually modeled using the advection-dispersion equation. Most existing models differ from each other mainly in the particle detachment and attachment terms. These models assume constant particle mobilization kinetics throughout the entire infiltration event. The hypothesis of a constant detachment rate together with a first-order kinetics can describe fairly well the mobilization in model porous media with model colloids (e.g., glass beads or washed sand with latexes) or in a few natural systems. This is the case

whenever the breakthrough (particle concentration vs. time) curves present a simple pattern, generally an initial peak followed by a decrease to an almost constant level [Schelde *et al.*, 2002; Jacobsen *et al.*, 1997]. However, far more complex breakthrough curves have been reported. Kjaergaard *et al.* [2004] studied intact macroporous soil columns with different clay content and initial humidity. They showed that for high-humidity/low-clay soils, the leached particle concentration increases during the whole or part of the experiment. For the most humid/lowest clay soil, an initial peak is first followed by a decrease and then by a subsequent increase in the concentration. Similar variations with time of the leached colloid concentration were also reported by Laegdsmand *et al.* [1999], Rousseau *et al.* [2004b], and Levin *et al.* [2006] in undisturbed soil columns.

[4] The reasons for the above mentioned fluctuations are still unclear. Shear stresses at the macropore walls during flow onset, as well as drainage of colloids trapped at the air-water interface have been put forward to explain the initial particle concentration peak [Rousseau *et al.*, 2004b; Laegdsmand *et al.*, 1999]. The observed variations during steady water flow regime are still unexplained. We suggest here that spatial and temporal variation of particle detachment rate might explain these fluctuations. They might be related to changes in interparticle interactions, successive detachment from superposed layers, variation of surface area exposed to water flow etc. For example, the detachment rate might drop if interparticle bonds increase, if more tightly attached particles become accessible to infiltrating water, if particles irreversibly attach to immobile phase, or if clogging of the flow paths occurs leading to filtration of the colloids. Conversely, weakening of interparticle bonds or

¹Laboratoire d'Etude des Transferts en Hydrologie et Environnement, UMR 5564, CNRS, INPG, IRD, UJF, Grenoble, France.

²Unité Climat, Sol et Environnement, Institut National de la Recherche Agronomique, Avignon, France.

³Laboratoire de Sciences de l'Environnement, ENTPE, Vaulx-en-Vélin, France.

detachment of a thin crust of particles that reveals poorly attached particles might increase the global detachment rate.

[5] So far, a few modeling efforts have been devoted to take some of these variations into account. Spatial variations of detachment kinetics were considered by *Haggerty and Gorelick* [1995] in a dual porosity model. Transfers between all immobile and mobile phases were assumed to occur simultaneously, and the parameters of the kinetics equations were assumed to be statistically or physically distributed. The preceding approach was adapted by *Saiers and Lenhart* [2003]: They hypothesized that release of colloids trapped in thin water films is the main mode of mobilization of artificial colloids in unsaturated sand column. They accounted for the dimensions and shape variability of the thin films by dividing them into different compartments, each having a critical moisture content above which the colloids are released. This critical moisture content distribution is determined by fitting the model to the experimental data.

[6] The variability of bacteria adhesion to porous media walls as a function of their residence time has been accounted for in bacterial transport models using residence time dependant detachment rates. *Johnson et al.* [1995] modeled bacterial release using a residence time dependant detachment function. Detachment is set to zero when adsorption duration exceeds a given residence time and bacteria become irreversibly adsorbed. This concept of residence time dependant detachment rate was generalized and formalized by *Ginn et al.* [2002].

[7] Additionally, it is enlightening to mention the strategy adopted to model the adsorption efficiency decrease with increasing coverage on collecting surfaces. A time-dependant attachment rate, more precisely, a “dynamic blocking function” was used. This function can take different mathematical expressions depending on the adsorption model considered [*Ryan and Elimelech*, 1996].

[8] Another possible limitation of most existing models is that they hypothesize a steady water flow regime. Therefore the detachment/attachment terms are defined only within this hypothesis. However, under natural conditions, unsteady water flow is rather the rule than the exception. As reported by *Saiers and Lenhart* [2003, paragraph 4], variations in pore water velocity accelerate “colloid release rates beyond that which would be predicted on the basis of steady flow experiments.” *Saiers and Lenhart* as well as *Jarvis et al.* [1999] considered that colloid detachment rates depend linearly on pore water velocity. Among the few other works considering water flow transient regimes, *Govindaraju et al.* [1995] on the other hand considered that the acceleration of pore fluid creates additional stresses proportional to the rate of pressure increase across the soil. They used three different equations to model the three parts of their experimental colloid breakthrough curves (initial rapid concentration increase, subsequent decrease and final constant concentrations).

[9] In this paper, in a modeling effort to capture the complex nature of *in situ* colloid detachment, we focus on the time variability of the mobilization using a time-dependent detachment rate within the source term of a classical convection-dispersion equation. More precisely, by analogy to the “blocking function” mentioned above, a “detachment efficiency function” is introduced. It is

related to the concentration of already mobilized particles through a mathematical function that reflects the different possible successive variations of particle detachment rate during infiltrations. This approach expands the *Johnson et al.* [1995] residence time dependant detachment rate concept, and it differs from the *Haggerty and Gorelick* [1995] and *Saiers and Lenhart* [2003] studies, which considered mobilization from different compartments at the same time. We also take into account the unsteady flow regime considering that colloid detachment, attachment, and transport processes occur during both transient and steady state water flow regimes. This led us to consider the additional inertial forces resulting from the water flux acceleration during flow onset. This approach is more general than *Govindaraju et al.* [1995] because a single equation is used to model the entire colloid breakthrough curve. Finally, preferential water transfer in macropores during both transient and steady state regimes are described using the kinematic dispersive wave approach developed by *Di Pietro et al.* [2003]. The proposed model is used to simulate particle mobilization and transport in two undisturbed soil columns submitted to rainfall events consisting of both unsteady and steady water flow regimes. We confront the numerical solutions with the experimental data and relate the model parameters favoring attachment and detachment of particles to the ionic strength of the incoming rainfall solution.

2. Soil Column Experiments

[10] This paper uses the experimental results already described by *Rousseau* [2003] and *Rousseau et al.* [2004b]. Two undisturbed soil columns (A and B) of the same dimensions (diameter = 0.3 m, height = 0.69 m) were extracted from the experimental field Les Closeaux (Versailles, France). The soil is a tilled loamy clay soil developed in loess deposit with properties given in Table 1. A set of 12 (3) infiltration experiments was performed on the soil column A (B). Rainfalls of controlled intensity and duration were simulated at the top of the core. Drainage was let free at the bottom of the column. During each infiltration, the weight of the outflowing solution and its turbidity were recorded and converted to drained water flux and eluted particle concentration respectively. Each experiment was performed after a draining period varying from 5 hours to 1 month. Two rainfall intensities (11 and 23 mm h⁻¹), and ionic strength varying from deionized water to 10⁻¹ M of MgCl₂ were tested. Experimental conditions of both columns A and B are given in Table 2.

3. Description of the Model

3.1. Water Flow Equation and Numerical Solution

[11] To simulate preferential water flow in macropores we adopted the kinematic-dispersive wave model developed by *Di Pietro et al.* [2003]. All capillary pores are assumed to be initially saturated. Under these conditions, infiltrating water rapidly flows through connected macropores and contributes to fast drainage. The kinematic-dispersive wave model assumes that the water flux $u(z, t)$ within the macropores is related to the macropore volumetric water content $\theta_m(z, t)$ by

$$u(z, t) = b \theta_m(z, t)^a + \nu_\theta \frac{\partial \theta_m(z, t)}{\partial t} \quad (1)$$

Table 1. Chemical, Physical, and Mineralogical Soil Properties

	Value
<i>Chemical Properties</i>	
Organic C, g kg ⁻¹	5.34
CaCO ₃ , g kg ⁻¹	2
PH	7.5
CEC, soil pH	12.6
Exchangeable Ca, cmol kg ⁻¹	12.31
Exchangeable Mg, cmol kg ⁻¹	0.55
Exchangeable K, cmol kg ⁻¹	0.40
Exchangeable Na, cmol kg ⁻¹	0.04
Free Fe, %	0.74
Ionic strength, mol l ⁻¹	1.17 10 ⁻²
<i>Physical Properties</i>	
Clay, %	20.65
Loam, %	61.02
Sand, %	17.56
Bulk density, g cm ⁻³	1.51
Porosity, cm ³ cm ⁻³	0.42
Water content at saturation, cm ³ cm ⁻³	0.41
Hydraulic conductivity at saturation, m s ⁻¹	1.9 10 ⁻⁴
<i>Mineralogical Properties</i>	
Chlorites, %	2.66
Smectites, %	43.35
Interstratified Illites/Smectites, %	6.69
Illites, %	37.74
Kaolinite, %	9.54

where $u(z, t)$ is the water flux at instant t and depth z , a is a macropore flow distribution index, b [mm h⁻¹] is a conductance term [Rousseau *et al.*, 2004a], and ν_θ [mm] is the water dispersion coefficient. By combining equation (1) with the continuity equation, Di Pietro *et al.* [2003] obtained the following nonlinear kinematic-dispersive equation for water flowing through noncapillary pores

$$\frac{\partial u(z, t)}{\partial t} + c[u(z, t)] \frac{\partial u(z, t)}{\partial z} = \nu[u(z, t)] \frac{\partial^2 u(z, t)}{\partial z^2} \quad (2)$$

[12] The functions $c[u(z, t)]$ and $\nu[u(z, t)]$ represent, respectively, the convective celerity and the dispersivity

responsible for the distortion of the advancing water front. They are defined by

$$c[u(z, t)] = ab^{1/a} u(z, t)^{a-1/a} \quad (3)$$

$$\nu[u(z, t)] = \nu_\theta c[u(z, t)] \quad (4)$$

[13] If the boundary condition is a square water pulse input at the surface, the solutions to equation (2) are traveling dispersive waves that fit well experimental drainage hydrographs. The typical shape of traveling wave solution is shown in Figure 1a along with associated experimental data. The hydrographs may be described in three main stages: a rapid transient increase (stage I), a plateau when a steady state is reached (stage II), and a steep decrease when the input flux is ceased (stage III). Figure 1b shows the corresponding stages on the breakthrough curve of the same experiment.

[14] In order to obtain the water flux profile, equation (2) is numerically solved using the finite differences method with an explicit discretization of the spatial derivatives and with the following initial and boundary conditions:

$$u(z, t) = 0, \quad z > 0, \quad t = 0, \quad t > t_s \quad (5)$$

$$u(z, t) = u_{in}(t), \quad z = 0, \quad 0 < t \leq t_s$$

where $u_{in}(t)$ is a square pulse water flow imposed on the top surface of the soil and t_s is the duration of the square pulse imposed on the top surface of the soil. Water flow parameters a , b , and ν_θ is estimated using Binary Genetic Algorithm optimization procedure between simulated and experimental fluxes [Holland, 1975; Goldberg, 1989].

[15] The volumetric water content profile within the macropores corresponding to the optimum parameters is obtained by numerically solving equation (1), using the finite differences method, with the following initial and boundary conditions:

$$\theta_m(z, t) = 0, \quad z > 0, \quad t = 0, \quad t > t_s \quad (6)$$

$$\theta_m(z, t) = \left(\frac{u_{in}(t)}{b}\right)^{\frac{1}{a}}, \quad z = 0, \quad 0 < t \leq t_s$$

Table 2. Experimental Conditions for Both Columns A and B^a

Rainfall Event Number	Time After Last Rainfall Event	Square Pulse Water Flow, mm h ⁻¹	Duration of Square Pulse, min	Incoming Solution Nature	Incoming Solution Ionic Strength, mol L ⁻¹	Eluted Particles Mass, mg
Col A3	1 month	10.98	228	MgCl ₂	1.64 × 10 ⁻³	263.48
Col A4	1 week	11.25	260	deionized water	7.02 × 10 ⁻⁶	1063.75
Col A5	1 week	11.13	225	MgCl ₂	1.71 × 10 ⁻³	365.54
Col A6	1 week	22.88	110	deionized water	1.25 × 10 ⁻⁵	2605.75
Col A8	5 hours	22.13	180	deionized water	1.57 × 10 ⁻⁵	5790.52
Col A10	1 week	10.94	185	MgCl ₂	1.40 × 10 ⁻³	1925.18
Col A12	1 week	11.20	180	MgCl ₂	1.30 × 10 ⁻¹	65.51
Col B1	1 month	24.48	202	deionized water	10 ⁻⁷	2090.79
Col B2	1 week	11.45	181	MgCl ₂	1.50 × 10 ⁻³	346.31
Col B3	1 day	11.48	120	MgCl ₂	1.54 × 10 ⁻³	223.05

^aRuns 1, 2, 7, 9, and 11 of column A are not reported because of technical incidents during infiltration. Nevertheless, the original number of rainfall event was conserved in order to reflect the history of the soil column.

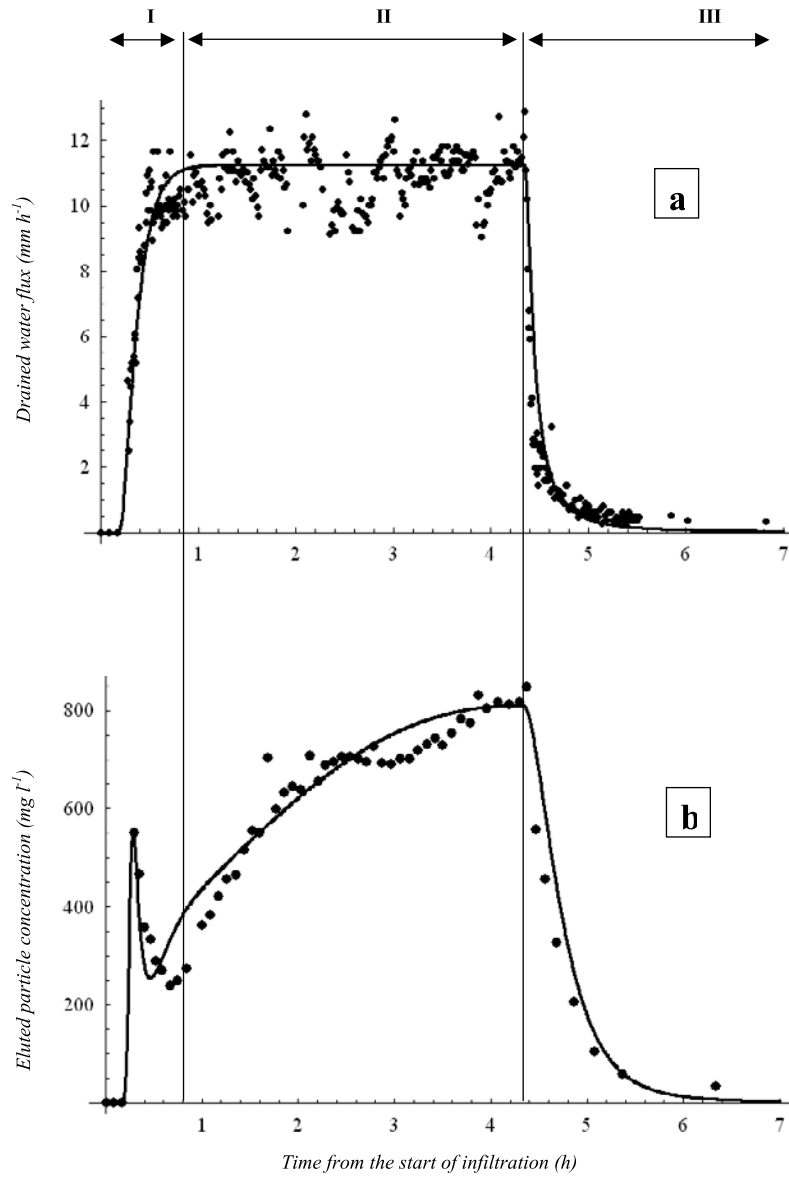


Figure 1. (a) Draining hydrograph and its characteristic stages I, II, and III. (b) Corresponding breakthrough curve. Circles show experimental data; line shows the simulation.

Both optimum water flux and volumetric water content profiles are subsequently used in the particle mobilization and transport equations.

3.2. Particle Mobilization and Transport Equations

[16] Particle transport in macropores is described by a convection-dispersion equation with source/sink terms:

$$\frac{\partial(\theta_m(z,t)C(z,t))}{\partial t} = -\frac{\partial(C(z,t)u(z,t))}{\partial z} + \frac{\partial}{\partial z} \left(\theta_m(z,t)D(z,t) \frac{\partial C(z,t)}{\partial z} \right) + S - P \quad (7)$$

where $C(z,t)$ [mg L⁻¹] is the mass concentration of particles in the flowing solution at depth z and time t , $D(z,t)$ [mm² h⁻¹] is the particle dispersion coefficient, S [mg L⁻¹ h⁻¹] is the source term that accounts for particle detachment, and

P [mg L⁻¹ h⁻¹] is the sink term that describes particle deposition along macropore walls.

3.2.1. Dispersion Coefficient

[17] Most existing studies concerning the dispersion coefficient in both natural and artificial media have been done under steady state water flow conditions. The dispersion coefficient is generally expressed [Nielsen *et al.*, 1986] by

$$D_p = \zeta D_0 + \lambda v_{pore}^\eta \quad (8)$$

where D_p [mm² h⁻¹] is a constant dispersion coefficient under steady flow conditions, ζ is the tortuosity, D_0 [mm² h⁻¹] is the molecular diffusion coefficient, λ [mm] is the dispersivity, v_{pore} [mm h⁻¹] is the pore water velocity, and η is a coefficient approximately equal to 1 for saturated systems. Pore water velocity is given by $v_{pore} = u_p/\theta_p$, where u_p and θ_p are the constant water flux and the volumetric

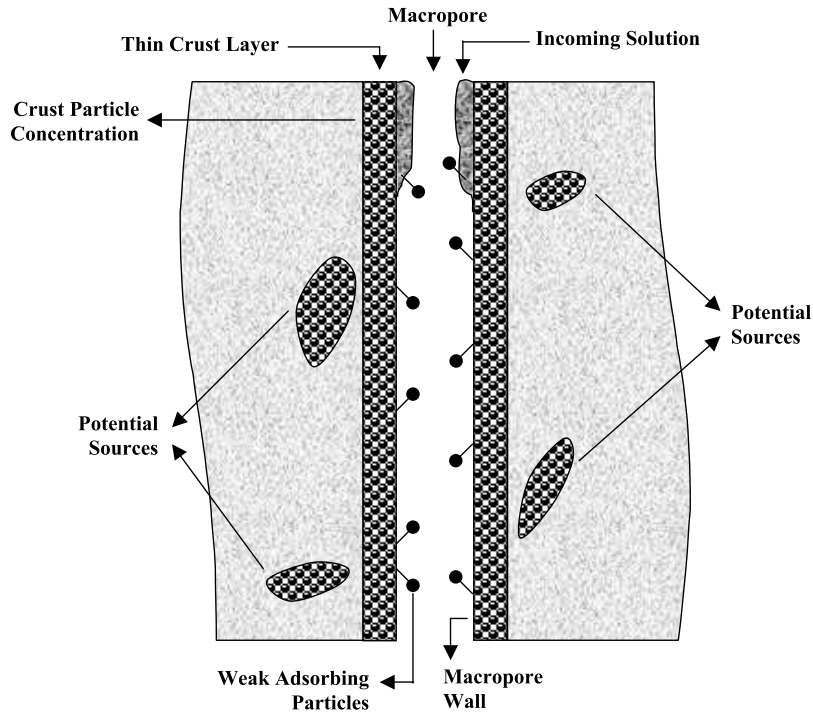


Figure 2. Model conception.

water content under steady state water flow conditions respectively. In our model, we consider that the dispersion coefficient $D(z, t)$ obeys Equation (8) even under unsteady and unsaturated water flow conditions. Bromide tracer experiments were performed on column A and B by Rousseau [2003] and Rousseau *et al.* [2004b]. Statistical moment analysis of the Br- breakthrough curves showed that the mean tracer residence time was 12 and 34 min in columns A and B, respectively. Residence times would have been more than 24 hours if calculated on the basis of Darcy's law. These observations indicate the presence of preferential flow, leading to rapid transport of solute through the macropore network, bypassing the soil matrix. Therefore flowing particles also bypass the matrix obstacles and tortuosity can be neglected. Equation (8) reduces to

$$D(z, t) = \lambda \frac{u(z, t)}{\theta_m(z, t)} \quad (9)$$

3.2.2. Sink Term

[18] The sink term P designates the deposit of transported particles along macropore walls. It is considered to be proportional to the particle concentration in the flowing solution according to

$$P = k_{att} \theta_m(z, t) C(z, t) \quad (10)$$

where k_{att} [h^{-1}] is an attachment rate coefficient.

3.2.3. Source Terms and Assumed Mechanisms for Particle Detachment

[19] We assume that the pool of particles that may potentially be mobilized can roughly be divided into three compartments, represented schematically in Figure 2: (1) a thin crust layer at the soil surface and along macropore

walls directly in contact with the incoming solution, (2) more weakly adsorbed particles that might be loosely deposited on macropore walls, and (3) other sources within the soil matrix that eventually start to release particles when exposed to flowing water. The considered mechanisms of particle detachment are the hydrodynamic (inertial) forces exerted by the flowing solution on the solid walls, and a combination of shear and physicochemical forces that counteract the cohesive forces between particles.

[20] Following Laegdsmand *et al.* [1999] and Rousseau *et al.* [2004b], who suggested that the inertial hydrodynamic forces created by water acceleration at the onset of the flow might be responsible for increased colloid mobilization, we hypothesize that the first source term S_1 is proportional to the water flux acceleration:

$$S_1 = k_{acc} \frac{\partial u(z, t)}{\partial t} \quad \text{with} \begin{cases} k_{acc} > 0, & \text{if } t \leq t_s \\ k_{acc} = 0, & \text{if } t > t_s \end{cases} \quad (11)$$

where k_{acc} [$\text{mg L}^{-1} \text{ h mm}^{-1}$] is a flux acceleration coefficient. This mechanism is effective only during the onset of infiltration (stage (I) of the drainage hydrograph). We hypothesize that it acts only on weakly adsorbed particles that have been loosened during the drying period.

[21] As for the thin crust layer compartment, we assume that the detachment of crust particles is mainly due to physicochemical interactions with the incoming solution following first-order kinetics. This mechanism is enhanced by shear forces along macropore walls due to the water flux, and thus the second source term S_2 is assumed to be proportional to $u(z, t)$. Additionally, the surface area of the crust in contact with the flowing solution depends on the water content within the macropores. Therefore S_2 is also proportional to $\theta_m(z, t)$. As mentioned in the introduction, we take into account the time variability of particle detach-

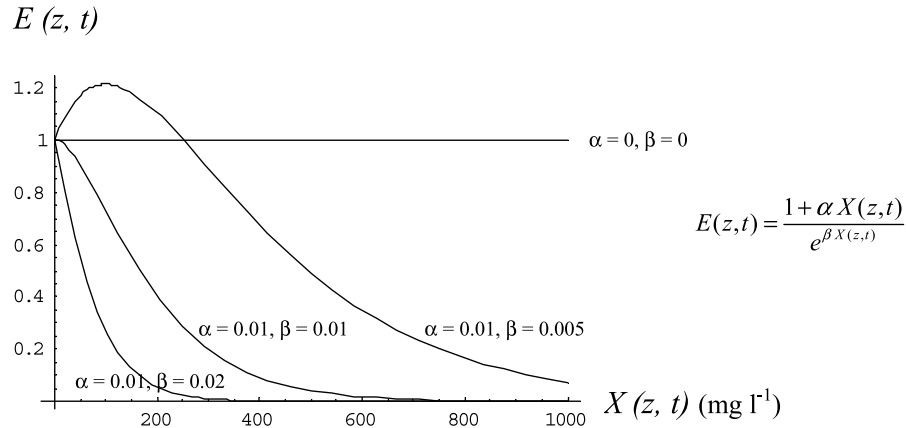


Figure 3. Different $E(z, t)$ behaviors as a function of $X(z, t)$ for four (α, β) parameter combinations.

ment introducing the detachment efficiency function $E(z, t)$ that will be detailed below. Finally, S_2 is expressed by

$$S_2 = k_{\text{det}} E(z, t) \theta_m(z, t) u(z, t) C^*(z, t) \quad (12)$$

where k_{det} [mm^{-1}] is the particle detachment coefficient, and $C^*(z, t)$ [mg L^{-1}] is the crust particle concentration. Similarly, attachment/detachment from macropore walls is expressed by

$$\frac{\partial C^*(z, t)}{\partial t} = -k_{\text{det}} E(z, t) \theta_m(z, t) u(z, t) C^*(z, t) + k_{\text{att}} \theta_m(z, t) C(z, t) \quad (13)$$

Equation (13) is based on an initial crust particle concentration $C_0^*(z)$ [mg L^{-1}] that undergoes changes during the infiltration event.

3.2.4. Detachment Efficiency: Definition and Mathematical Formulation

[22] In this study we consider that the experimentally observed fluctuating colloid breakthrough curves may be related to temporal and spatial variations of detachment rate. Our goal here is not to study the small-scale spatial variations of local detachment rates (resulting for example from local variability of inter particles forces) as done by *Haggerty and Gorelick* [1995]. We rather focus on the temporal variability of the detachment rate which is not taken into account in the aforementioned study.

[23] In the soil, particles in contact with water may not all detach simultaneously. Some are more tightly bound than others and might be detached only after a while: the detachment is kinetically limited. The physical processes leading to this delay may include dissolution of cements binding the particles together or change of inter particle ionic strength by ion diffusion. Furthermore, during the infiltration, the total number of particles that can be potentially detached in the soil column may vary with the total surface area of soil in contact with flowing water, as particles are removed from or deposited onto the pores walls, and as pores become clogged or unclogged. These phenomena may result in temporal variations of the detachment rate and strongly depend on the amount of already detached particles. For example the detachment of some particles can enhance the detachment of others if the

detached particles let colloids flow through a previously clogged pore, or if they loosen the connections between neighboring particles. Conversely, the detachment of some particles may disfavor the detachment of others (e.g., detached particles clog some water conducting pores yielding to filtration).

[24] In this paper, we model the temporal variations of the detachment rate introducing a “detachment efficiency function” $E(z, t)$. Since these variations depend on the amount of already detached particles, so does $E(z, t)$. The detachment efficiency function depends thus on time through a variable $X(z, t)$ describing the history of detachment process. Quantitatively, $X(z, t)$ [mg L^{-1}] is the cumulative concentration of particles detached at time t :

$$X(z, t) = \int_0^t k_{\text{det}} E(z, \tau) \theta_m(z, \tau) u(z, \tau) C^*(z, \tau) d\tau \quad (14)$$

[25] The possible variations of detachment rate suggest the following shape variations of $E(z, t)$: (1) constant $E(z, t)$ value for variable $X(z, t)$ reflecting a classical first-order kinetics, (2) continuous decrease of $E(z, t)$ with increasing $X(z, t)$ (detachment of some particles disfavors the detachment of others), and (3) increase of $E(z, t)$ with increasing $X(z, t)$ (detachment of some particles enhances the detachment of others) followed by a decrease for large $X(z, t)$ values. This decrease is due to the fact that particles cannot be offered infinitely to the soil solution and, after an infinite mobilization process, particles stocks are exhausted yielding $E(z, t) \rightarrow 0$ if $X(z, t) \rightarrow \infty$. In order to satisfy these conditions, we propose to relate $E(z, t)$ to $X(z, t)$ through the following function:

$$E(z, t) = \frac{1 + \alpha X(z, t)}{e^{\beta X(z, t)}} \quad (15)$$

where α [$\text{mg}^{-1} \text{L}$] and β [$\text{mg}^{-1} \text{L}$] are two positive parameters. Figure 3 shows the behaviors of $E(z, t)$ as a function of $X(z, t)$ for four (α, β) parameter combinations. $E(z, t)$ shows a maximum for $X(z, t) = X_{\text{max}}(z, t) = (\alpha - \beta) / (\alpha\beta)$. Three cases may be considered according to the relative values of α and β : (1) $\alpha = \beta = 0$, this case reduces to a classical first-order kinetics with constant detachment efficiency $E(z, t) = 1$; (2) $0 < \alpha < \beta$, $X_{\text{max}}(z, t)$ is strictly positive, $E(z, t)$ increases, reaches a maximum at $X_{\text{max}}(z, t)$

and then decreases for $X_{\max}(z, t) < X(z, t)$; (3) $0 < \alpha \leq \beta$ in this case, $X_{\max}(z, t)$ is either null or negative, and $E(z, t)$ always decreases for increasing positive $X(z, t)$ values.

3.2.5. Numerical Solution

[26] Equations (7), (13), (14), and (15) form the particle mobilization and transport model. They are numerically solved in a simultaneous way using the finite differences method with an implicit discretization of spatial derivatives for the convection-dispersion equation, and with the following initial and boundary conditions:

$$\begin{aligned} C(z, t) &= 0, & z > 0, & t = 0 \\ C^*(z, t) &= C^*o(z), & z > 0, & t = 0 \\ X(z, t) &= 0, & z > 0, & t = 0 \end{aligned} \quad (16)$$

[27] Particle transport model parameters k_{acc} , k_{att} , k_{det} , α , and β are estimated using binary genetic algorithm optimization procedure between simulated and experimental eluted particle concentrations.

4. Parameter Estimation–Sensitivity Analysis

4.1. Dispersivity Estimation

[28] In field studies, the average dispersivity λ is about 3 cm, which is larger than the λ measured in laboratory soil columns [Bresler and Laufer, 1974; Nielsen and Biggar, 1962]. According to Jury *et al.* [1991], typical values of λ for soil columns range from 0.5 to 2 cm. The maximum dispersivity value used by Bresler and Dagan [1983] was 3 cm, which is in the range of the studies reviewed by Sposito *et al.* [1986]. For our soil columns, we consider a medium λ value in the range given by the literature: $\lambda = 1.5$ cm.

4.2. Initial Estimation of the Macropore Crust Particle Concentration

[29] The initial macropore crust particle concentration can be (1) calibrated for each single rainfall event or (2) fixed at the beginning of the first rainfall event, the final crust concentration state of each rainfall event being thus considered as the initial concentration state of the following event. The first alternative is commonly used in the literature [Roy and Dzombak, 1996; Jacobsen *et al.*, 1997; Schelde *et al.*, 2002] but can lead to initial concentration values for some rainfall events that are higher than that of previous events. We adopted the second alternative which is more suitable to describe successive rainfall events. We first suppose that the primitive macropore crust particle concentrations in columns A and B are identical because the two soil columns were extracted near each other, and call this value C_{prim}^* . We then estimate this value: it is at least greater than the cumulative mass of eluted particles during all simulated rainfall events divided by the column soil volume. On the basis of eluted particles mass for column A (Table 2), we get $C_{prim}^* > 450$ mg L⁻¹. In order to avoid overestimation of C_{prim}^* , we decided to adopt the lowest value of C_{prim}^* higher than 450 mg L⁻¹ that can lead to successful simulations of the set of successive rainfall events. C_{prim}^* values of 500 and 1000 mg L⁻¹ were tested but they were not able to reproduce the whole set of rainfall events. We thus chose $C_{prim}^* = 1500$ mg L⁻¹. Studying in situ colloid release from intact soil columns (the same context as in this study), Jacobsen *et al.* [1997] found that the calibrated initial concentration on the macropore wall

for particles smaller (respectively greater) than 10 μ m varied between 490 and 4000 mg L⁻¹ (respectively between 100 and 180 mg L⁻¹). In our experiments, the predominant size of particles in the outflow solution is approximately 0.45 μ m [Rousseau *et al.*, 2004b]. Our estimate of C_{prim}^* concurs thus with Jacobsen *et al.* [1997] values.

4.3. Sensitivity Analysis

[30] Water flow parameters as well as particle transport parameters, can take any real positive value. To limit the parameters range of variations, interval values must be defined for each parameter. Moreover, inside these intervals, very close parameter values produce almost the same simulations. We prevent the GA from performing useless evaluations by dividing intervals into small steps in such a way that the simulated curve is sensitive to a one step parameter change. Parameters sensitivity analysis was used to determine the size of each interval.

4.3.1. Water Flow Parameters

[31] On the basis of existing literature values [Di Pietro *et al.*, 2003; Rousseau, 2003] and on the sensitivity analysis done by Di Pietro *et al.* [2003], we defined the following parameter intervals for water flow parameters a , b , and ν_θ : $a \in [1, 4.1]$ with a step of 0.1, $b \in [10^5, 10^{11.2}]$ with a step of $10^{0.2}$ [mm h⁻¹], and $\nu_\theta \in [150, 900]$ with a step of 50 [mm].

4.3.2. Particle Transport Parameters

[32] In this study, k_{det} is expressed in [mm⁻¹], while in the literature it is generally expressed in [h⁻¹]. We compare our detachment coefficient with other existing literature values, by multiplying k_{det} [mm⁻¹] by the water flow imposed on the top surface of the soil $u_m(t)$ [mm h⁻¹] to obtain $k_{det}u_m(t)$ expressed in [h⁻¹]. Literature values for colloids attachment/detachment rates [Roy and Dzombak, 1996; Jacobsen *et al.*, 1997; Kretzschmar *et al.*, 1997; Camesano *et al.*, 1999; Zhuang *et al.*, 2004] show that the detachment (respectively attachment) rates vary between 0.31 and 50 h⁻¹ (respectively 0.14 and 100 h⁻¹). These constraints were adopted for our attachment/detachment rate parameters. Consequently, we let both $k_{det}u_m(t)$ and k_{att} vary between 0.1 and 75 h⁻¹.

[33] Sensitivity analysis was done for particle transport parameters (Figure 4) in order to determine both parameter interval steps and the influence of each parameter on the simulated breakthrough curve. Figures 4a–4e shows parameter increments that can produce appreciable changes in simulation curves. It was noticed that, to be sensitive, parameter increment must increase along with the increasing parameter value. We thus chose increment steps in the order of the decimal of parameter value: a parameter value of 0.2 for example will be incremented by 0.01 to yield 0.21, and a parameter value of 3 will be incremented by 0.1 to yield 3.1. Particle transport parameters were thus varied inside the following intervals: $\alpha \in [0, 0.0001, \dots, 0.75]$ [mg⁻¹ L], $\beta \in [0, 0.0001, \dots, 0.75]$ [mg⁻¹ L], $k_{acc} \in [0, 0.001, \dots, 7.5]$ [mg L⁻¹ h mm⁻¹], $k_{att} \in [0, 0.1, \dots, 75]$ [h⁻¹], and $k_{det}u_m(t) \in [0, 0.1, \dots, 75]$ [h⁻¹].

5. Results and Discussion

5.1. Water Flow: Comparisons Between Simulations and Experimental Data

[34] The results of the water flux simulations (Figure 5) show the following.

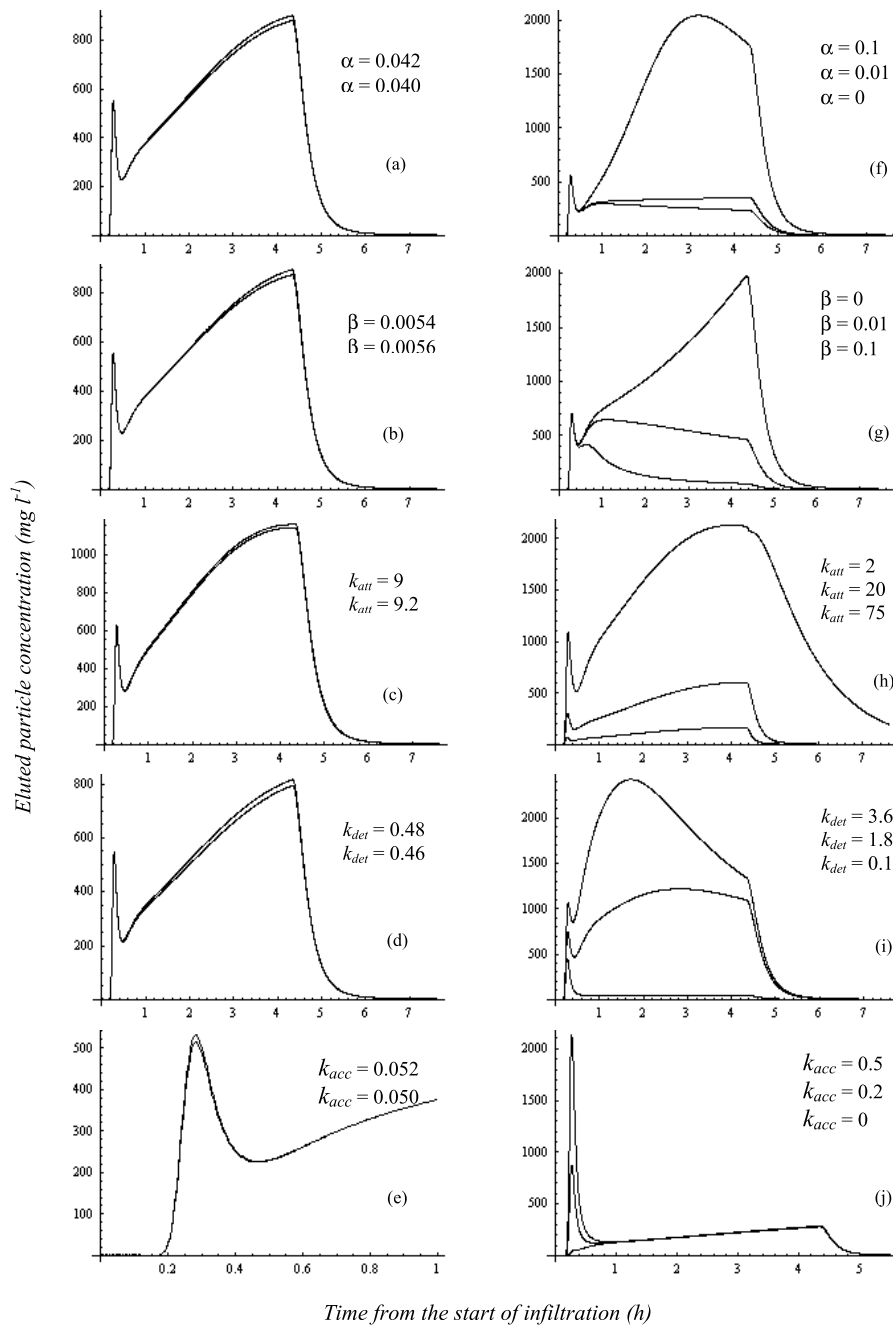


Figure 4. (a–j) Sensitivity analysis for particle transport model parameters varying in both fine and large interval values. The order in which parameters are written (from top to bottom) corresponds to that of the associated curves. Figure 4e was plotted between 0 and 1 h in order to show the peak variation.

[35] 1. Stage I of the hydrograph corresponds to rapid flow increase is well simulated. The model correctly predicts the breakthrough of the wetting front. The dispersive phenomenon which is expressed by the smooth curvature at the end of stage I is well represented in all columns. This reinforces the hypothesis of *Di Pietro et al.* [2003] concerning the dispersion of the wetting front due to variation in pore water velocities in different pores.

[36] 2. Stage II corresponds to the steady regime reflects the square pulse water flow $u_{in}(t)$ imposed on the column surface.

[37] 3. Stage III corresponds to the turn off of irrigation. The tail of the falling limb is well represented, except for column A, experiment 12 (hereinafter experiments will be abbreviated as, e.g., Col A12), Col B1, and Col B3 where simulations underestimate the experimental water flux.

[38] Water flow parameters estimated by the GA optimization procedure (Table 3) indicate that a varies between 2.1 and 3.8, b varies between $10^{5.6}$ and $10^{10.2}$ mm h⁻¹, and v_0 varies between 200 and 800 mm. These values are in good agreement with values found in literature [*Di Pietro et al.*, 2003; *Rousseau*, 2003; *Rousseau et al.*, 2004a].

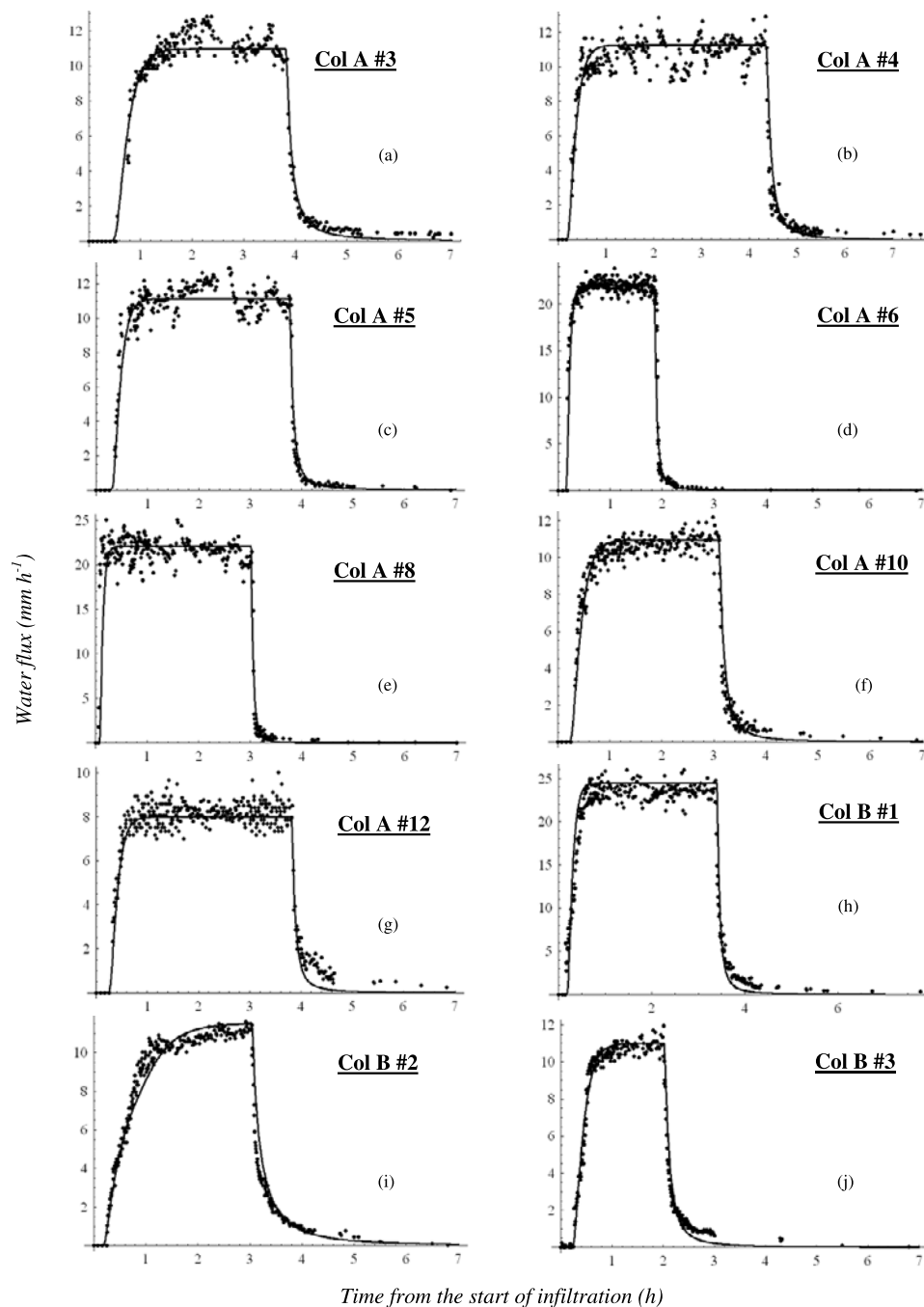


Figure 5. Water flux simulations. Circles show experimental data; line shows the simulation.

5.2. Particle Transport: Relation to Existing Modeling Efforts

[39] *Johnson et al.* [1995] modeled bacterial detachment kinetics in homogeneous systems using a dynamic rate of detachment, where bacterial release (source term) is set to zero after a specified residence time. In the same way, in natural systems, detachment efficiency can drop due to pores clogging and subsequent particle filtration for example. Conversely, particles that were not yet on the water flow path can later start to be mobilized. Also, water flow can weaken the cohesion of particles that were previously too tightly bound to be mobilized. This means that source terms that were not taken into account will be different from

zero at subsequent times. These two tendencies (activation/deactivation of source term) coexist continuously in natural systems during the same rainfall event, and the observed concentration of leached particles is the result of these opposite phenomena. Our concept of a detachment efficiency $E(z, t)$ is capable of reflecting and summarizing the essential of this dynamic with only two adjustable parameters.

[40] The use of mathematical functions to describe parameter variability is ubiquitous in transport literature. *Ginn* [2000b] illustrated the use of the exposure time theory [*Ginn*, 2000a] expanding and refining *Johnson et al.*'s [1995] work on residence time dependant detachment rate:

Table 3. Optimized Values of Water Flow and Particle Transport Parameters

Rainfall Event Number	Water Flow Parameters			Particle Transport Parameters				
	a	b , mm h ⁻¹	ν_θ , mm	k_{acc} , mg L ⁻¹ h mm ⁻¹	k_{att} , h ⁻¹	$k_{det} u_{in}(t)$, h ⁻¹	α , mg ⁻¹ L	β , mg ⁻¹ L
Col A3	3.2	10 ⁸	450	0.65	61	7.46	0.0031	0.0023
Col A4	2.1	10 ⁶	400	0.045	8	2.25	0.04	0.008
Col A5	3.8	10 ^{10.2}	600	0.084	4	0.88	0.0093	0.0015
Col A6	2.5	10 ^{7.8}	200	0.017	6.8	14.87	0.036	0.013
Col A8	2.6	10 ^{8.6}	450	0	9.8	61.96	0.009	0.0052
Col A10	2.7	10 ⁷	800	0.52	19	27.35	0.0035	0.0023
Col A12	3.5	10 ^{9.8}	700	0.062	9.7	4.14	0.0045	0.6
Col B1	2.8	10 ^{7.8}	400	0.001	10	2.25	0.052	0.0047
Col B2	2.1	10 ^{5.6}	650	0.03	9.9	1.94	0.005	0.0037
Col B3	2.5	10 ^{6.6}	700	0.003	8	1.60	0.015	0.0085

The variations of detachment rate with bacteria residence time onto the porous media material are modeled using a two parameter smoothed version of the Heaviside function. *Weiss et al.* [1998] observed that the resistance to desorption of latex particles from a glass surface increases with adhesion duration. They used a two parameter gamma distribution of the potential well depth at the binding sites to calculate the desorption rate distribution causing the observed adhesion time distribution. *Haggerty and Gorelick* [1998] used a two parameters lognormal distribution to model the variability of organic compounds diffusion coefficient in unsaturated porous media. *Grolimund et al.* [2001] studied colloid release from intact soils using generalized exponential and power law type distributions of detachment rate to describe experimental data that could not be modeled by first-order kinetics. In these studies, experimental data are better described using statistical distributions of the relevant rate than simple first-order kinetics. In the same

way, in this study we chose to describe the time variability of colloid detachment using the two parameter $E(z, t)$ function. The proposed mathematical form of $E(z, t)$ (equation (15)) allows to model colloid breakthrough curves that cannot be described by a first-order kinetics when parameters α and β are different from zero, but can be reduced to a first-order kinetics when $\alpha = \beta = 0$. Other mathematical forms of the detachment efficiency can be tested in the future to check if they can better describe the experimental curves.

5.3. Particle Transport: Comparisons Between Simulations and Experimental Data

[41] Classical first-order kinetic ($\alpha = \beta = 0$) along with no flux acceleration ($k_{acc} = 0$) during flow onset was first used to simulate the experimental data. The initial peak as well as the subsequent rise in particle concentration are not captured by this model (e.g., Col A4 in Figure 6a). Adjustment of the

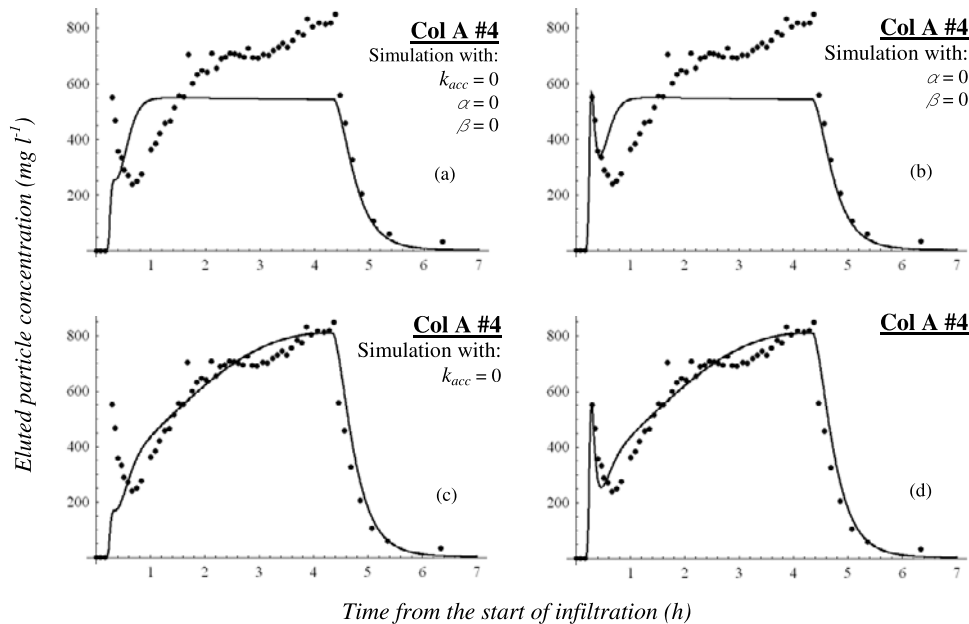


Figure 6. (a) Simulation using $k_{acc} = 0$ [mg l⁻¹ h mm⁻¹], $\alpha = 0$ [mg⁻¹ L], and $\beta = 0$ [mg⁻¹ L]. (b) Simulation using $\alpha = 0$ [mg⁻¹ L], $\beta = 0$ [mg⁻¹ L], and best fit for $k_{acc} = 0.045$ [mg l⁻¹ h mm⁻¹]. (c) Simulation using $k_{acc} = 0$ [mg l⁻¹ h mm⁻¹], best fit for $\alpha = 0.04$ [mg⁻¹ L], and $\beta = 0.008$ [mg⁻¹ L]. (d) Model simulation, best fit for $k_{acc} = 0.045$ [mg l⁻¹ h mm⁻¹], $\alpha = 0.04$ [mg⁻¹ L], and $\beta = 0.008$ [mg⁻¹ L]. Circles show experimental data; line shows the simulation. Here k_{det} and k_{att} were free to vary for all simulations.

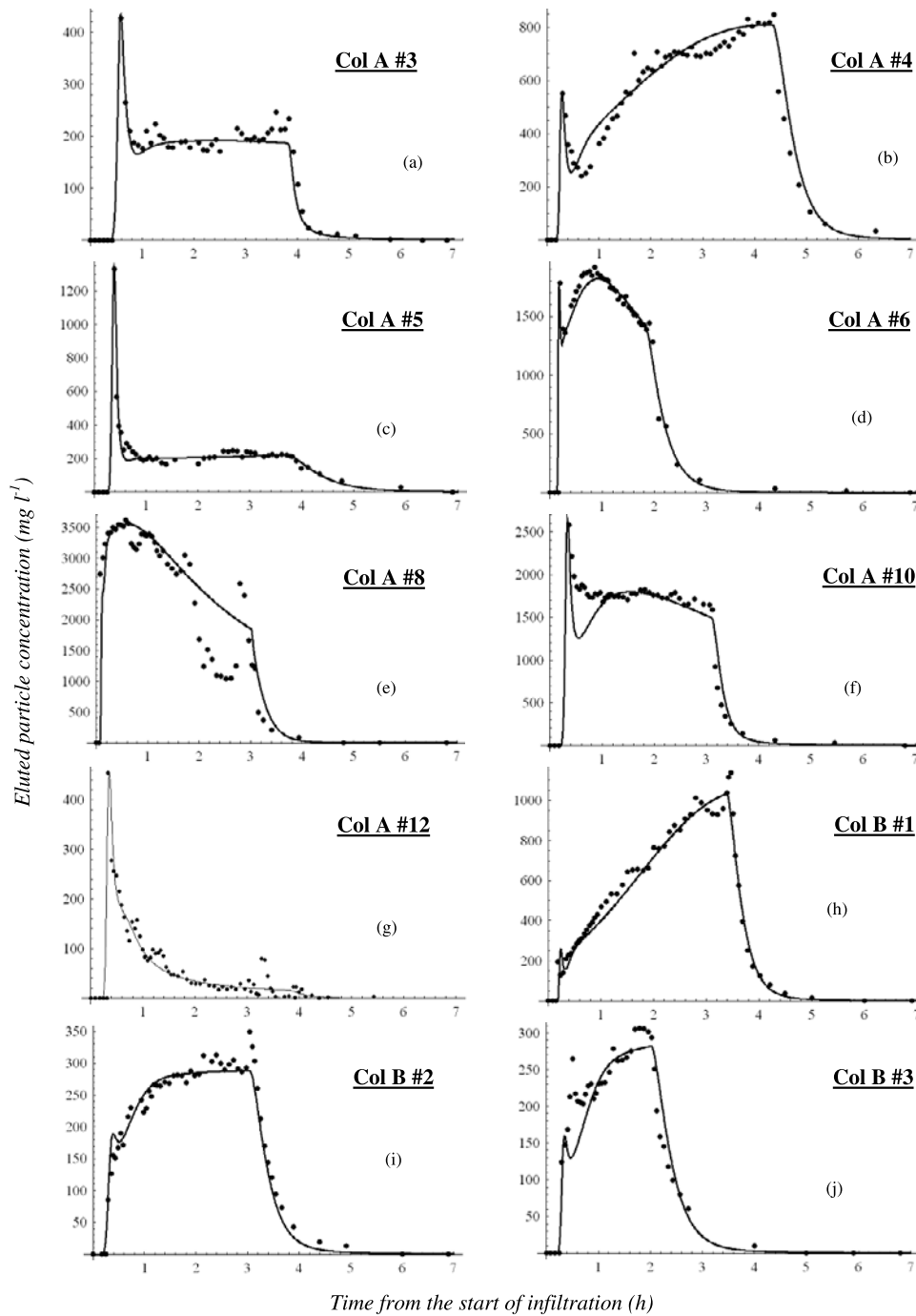


Figure 7. Particle transport simulations. Circles show experimental data; line shows the simulation.

k_{acc} parameter allows a good reproduction of the initial peak (Figure 6b) while the use of the efficiency function in the model allows a better simulation of the colloid concentration increase during the steady flow regime (Figure 6c). Finally, taking into account the acceleration effect as well as the efficiency function yields a good simulation of experimental data (Figure 6d). The model was fitted to all experimental breakthrough curves for columns A and B. The model ability to describe experimental data for the three stages of the breakthrough curves (Figure 7) is discussed below.

[42] 1. In stage I the adjustment of the k_{acc} parameter allows a good reproduction of the peak and the steep rising limb of the colloid breakthrough curve every time a peak is present. Conversely, the absence of peak in Col A8 and all column B infiltrations is reproduced with values of k_{acc} close to zero. Govindaraju *et al.* [1995] attributed the rising limb of their breakthrough curves to the temporal variation of the pressure applied across the soil. Their model yielded premature particle breakthrough and overestimated the initial peak compared to their experimental data. Our simulations describe this part of the curve better than the

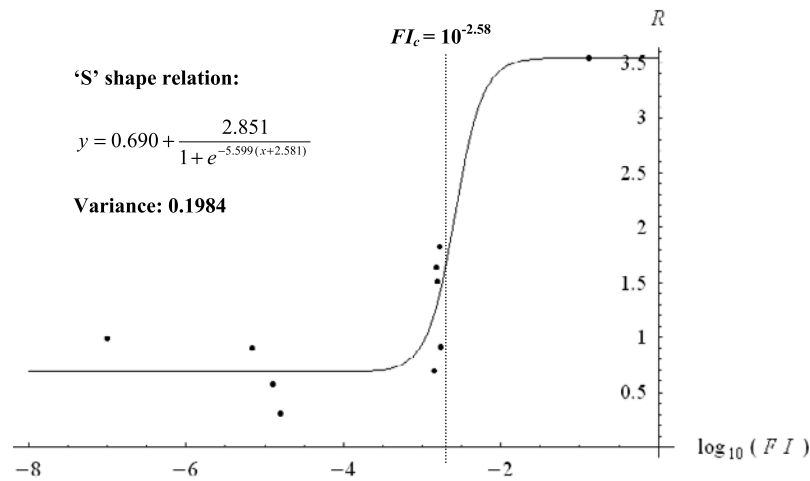


Figure 8. Fermi-type relation between R ratio and the base 10 logarithm of the incoming solution ionic strength FI .

simulations of Govindaraju *et al.* [1995] and show that the hypothesis of particle mobilization due to flux acceleration is more appropriate to reflect stage I than the hypothesis of temporal variation of the pressure applied across the soil.

[43] 2. Stage II corresponds to the steady water flow regime and exhibits different particle leaching trends with time: (1) an increasing eluted particle concentration (Col A4, Col B1, and Col B2) reflecting the eventuality that the detachment of some particles promotes the detachment of others as time is running, (2) an increase followed by a decrease in eluted particle concentration (Col A6), or even a continuous decrease in eluted particle concentration (Col A10 and Col A12), as for example, more tightly attached particles become in contact with flowing water, or particles get filtrated due to pore clogging, and (3) a constant eluted particle concentration (Col A3, Col A5) reflecting classical first-order kinetics. These patterns are well simulated except for infiltration Col A4 and Col A10 where the eluted particle concentration is respectively overestimated and underestimated at the beginning of stage II.

[44] 3. In stage III, after the infiltration turn off, the convective transport gradually stops, resulting in a decreasing flow rate and in a fast decrease in particle concentration flux as well. The falling limb is well reproduced for all rainfall events.

[45] Particle transport parameters estimated by the GA optimization procedure are given in Table 3. The detachment rate varied between 0.88 and 62 h^{-1} with a majority of values below 10 h^{-1} . These values are comparable with those found by Jacobsen *et al.* [1997] in intact macroporous soil columns and Roy and Dzombak [1996] in natural sands for in situ colloid mobilization. The attachment rate varied between 4 and 61 h^{-1} with a majority of values below 10 h^{-1} . Published attachment rate estimates obtained in experimental situations close to ours are scarce, but our values have the same order of magnitude as the estimates obtained with colloids introduced in repacked soil columns [e.g., Kretzschmar *et al.*, 1997; Zhuang *et al.*, 2004]. While the attachment rate estimates show a tendency toward a value around 9 h^{-1} (Table 3), the detachment rate estimates are more scattered.

[46] In order to predict the preferential transport of particles through undisturbed natural soils, model param-

eters should be related to experimental conditions and to soil properties. In our infiltration experiments, the main changing experimental conditions were the water flux and the incoming solution ionic strength. Physicochemical attachment/detachment on macropore walls (equation (13)) is influenced by the ionic strength of the incoming solution, and so will be the particle transport parameters (k_{att} , k_{det} , α , and β). Sensitivity analysis shows that increasing k_{att} and β enhances particle deposit (Figures 4g and 4h), while increasing k_{det} and α favors particle release (Figures 4f and 4i). The ratio R [mm h^{-1}] of parameters promoting particle deposit to parameters promoting particle release is

$$R = \frac{\beta k_{att}}{\alpha k_{det}} \quad (17)$$

R was calculated for all experiments and plotted versus the ionic strength FI . As a first step toward the prediction of the functional dependence of R on FI , we adjusted data points by a Fermi-type function (Figure 8) according to

$$\frac{R - R_{min}}{R_{max} - R_{min}} = \frac{1}{1 + e^{-\delta(\log_{10}(FI) - \log_{10}(FI_c))}} \quad (18)$$

where $R_{min} = 0.690 \text{ mm h}^{-1}$ and $R_{max} = 2.851 \text{ mm h}^{-1}$ are respectively minimum and maximum values of R ratio, $\delta = 5.599$ is a form parameter, FI [M] is the ionic strength of the incoming solution, and $FI_c = 10^{-2.581}$ M is the critical ionic strength threshold around which R ratio passes from R_{min} to R_{max} . To assert relation (18), more infiltration tests need to be done with varying ionic strengths, mainly for high values of FI . Relation (18) reflects the fact that lower incoming solution ionic strength enhances particle leaching. It is also consistent with the hypothesis proposed by Khilar and Fogler [1984], suggesting that ionic strength acts on particle mobilization as a threshold mechanism.

6. Validation of the Model

[47] In order to test the validity of the model, two predictive simulations were run for Col A5 (Figure 9a) and Col B3 (Figure 9b) using all five particle transport

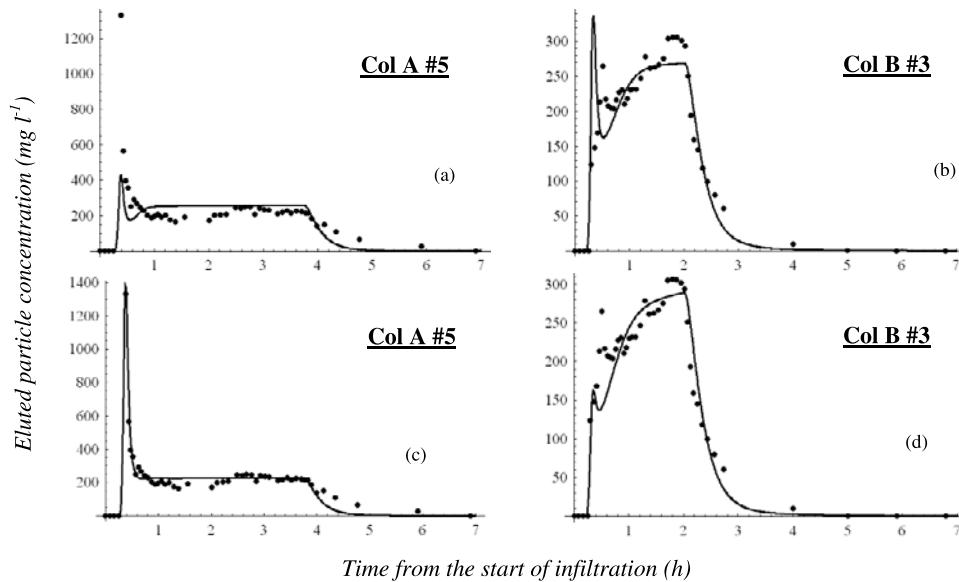


Figure 9. Validation of the model. (a) Result of the prediction for Col A5 using particle transport parameters calibrated from Col B2. (b) Result of the prediction for Col B3 using particle transport parameters calibrated from Col B2. (c) Result of the simulation for Col A5 using k_{att} and k_{det} parameters calibrated on Col B2 and k_{acc} , α , and β parameters calibrated from Col A5. (d) Result of the simulation of Col B3 using k_{att} and k_{det} parameters calibrated from Col B2 and k_{acc} , α , and β parameters calibrated from Col B3. Circles show experimental data; line shows the simulation.

parameters (k_{acc} , k_{det} , k_{att} , α , and β) calibrated on Col B2. These columns have the same experimental conditions: square pulse water flow about 11 mm h^{-1} and incoming solution ionic strength approximately $1.5 \cdot 10^{-3} \text{ M}$. While stages II and III of the breakthrough curves are satisfactory predicted, the concentration peak is underestimated in Col A5 and overestimated in Col B3. This suggests that k_{acc} parameter is sensitive to macropore network differences between one soil column and another, as well as macropore network changes between one infiltration event and another on the same soil column.

[48] Although Col A5 and Col B3 have the same experimental conditions as Col B2, they do not have the same history. The columns have undergone a different number of rainfall events. Therefore, if we consider that k_{att} and k_{det} are closely related to experimental conditions (such as nature of the soil, incoming solution ionic strength, rainfall intensity) while k_{acc} , α and β depend more on macropore network structure and column history, we can run a simulation of Col A5 and Col B3 using the k_{att} and k_{det} parameters calibrated on Col B2 and k_{acc} , α and β parameters calibrated on Col A5 (Figure 9c) and Col B3 (Figure 9d). The predictions are satisfactory. This raises the problems of the quantification of macroporosity in soils, and its changes with soil history.

7. Conclusions

[49] In this study, we modeled mobilization and transport of particles in natural macroporous soils under unsaturated conditions. We used the kinematic dispersive wave approach to model macropore water flow and introduced a time-dependent source term to describe variability of particle release from macropore crust. The KDW model described well the behavior of water flux, showing thus

the capacity of the kinematic dispersive waves to describe preferential water flow in structured natural soils. The particle transport model gave very satisfactory simulations of eluted particle concentrations with only two more parameters than contained in models based on a first-order kinetics. The validation of the model was tested on two predictive simulations. It showed that the initial concentration peak can hardly be simulated without a calibration of the k_{acc} parameter. The ability of the model to predict particle transport requires the relation of all its parameters to experimental conditions or to soil properties. A step has been done in this direction by relating the ratio R to the ionic strength of the incoming solution FI . To assert this relation, further infiltration experiments must be carried out with incoming solution ionic strength around the FI_c threshold. Additionally, quantification of the soil macroporosity and its variations in time would help predicting particle mobilization and transport through a better estimation of macroporosity dependant parameters.

[50] **Acknowledgments.** We wish to thank Yves Dudal from INRA-Avignon and Jean-Paul Gaudet and Jean-François Daïan from LTHE Grenoble for many helpful suggestions and comments. This work was partially supported by the ECCO-PNRH ("Programme National de Recherches en Hydrologie," French Hydrological Research Program) on the project "Particules."

References

- Bresler, E., and G. Dagan (1983), Unsaturated flow in spatially variable fields: 2. Application of water flow models to various fields, *Water Resour. Res.*, 19, 421–428.
- Bresler, E., and A. Lauffer (1974), Anion exclusion and coupling effects in nonsteady transport through unsaturated soils. II. Laboratory and numerical experiments, *Soil Sci. Soc. Am. Proc.*, 38, 213–218.
- Camesano, T. A., K. M. Unice, and B. E. Logan (1999), Blocking and ripening of colloids in porous media and their implications for bacterial transport, *Colloids Surf. A*, 160, 291–308.

- Di Pietro, L., S. Ruy, and Y. Capowicz (2003), Predicting water flow in soils by traveling-dispersive waves, *J. Hydrol.*, 278(1–4), 64–75.
- Ginn, T. R. (2000a), On the distribution of multicomponent mixtures over generalized exposure time in subsurface flow and reactive transport: Theory and formulations for residence-time-dependent sorption/desorption with memory, *Water Resour. Res.*, 36(10), 2885–2893.
- Ginn, T. R. (2000b), On the distribution of multicomponent mixtures over generalized exposure time in subsurface flow and reactive transport: Batch and column applications involving residence-time distributions and non-Markovian reaction kinetics, *Water Resour. Res.*, 36(10), 2895–2903.
- Ginn, T. R., B. D. Wood, K. E. Nelson, T. D. Scheibe, E. M. Murphy, and T. P. Clement (2002), Processes in microbial transport in the natural subsurface, *Adv. Water Resour.*, 25, 1017–1042.
- Goldberg, D. E. (1989), *Genetic Algorithms in Search, Optimization, and Machine Learning*, Addison-Wesley, Boston, Mass.
- Govindaraju, R. S., L. N. Reddi, and S. K. Kasavaraju (1995), A physically based model for mobilization of kaolinite particles under hydraulic gradients, *J. Hydrol.*, 172, 331–350.
- Grolimund, D., K. Barmettler, and M. Borkovec (2001), Release and transport of colloidal particles in natural porous media: 2. Experimental results and effects of ligands, *Water Resour. Res.*, 37(3), 571–582.
- Haggerty, R., and S. M. Gorelick (1995), Multiple-rate transfer for modeling diffusion and surface reactions in media with pore-scale heterogeneity, *Water Resour. Res.*, 31(10), 2383–2400.
- Haggerty, R., and S. M. Gorelick (1998), Modeling mass transfer processes in soil columns with pore-scale heterogeneity, *Soil Sci. Soc. Am. J.*, 62, 62–74.
- Holland, J. H. (1975), *Adaptation in Natural and Artificial Systems*, Univ. of Mich. Press, Ann Arbor.
- Jacobsen, O. H., P. Moldrup, C. Larsen, L. Konnerup, and L. W. Petersen (1997), Particle transport in macropores of undisturbed soil columns, *J. Hydrol.*, 196, 185–203.
- Jarvis, N. J., K. G. Villholth, and B. Ulen (1999), Modelling particle mobilization and leaching in macroporous soil, *Eur. J. Soil Sci.*, 50, 621–632.
- Johnson, W. P., K. A. Blue, B. E. Logan, and R. G. Arnold (1995), Modeling bacterial detachment during transport through porous media as a residence-time-dependent process, *Water Resour. Res.*, 31(11), 2649–2658.
- Jury, A. W., W. R. Gardner, and W. H. Gardner (1991), *Soil Physics*, 5th ed. John Wiley, Hoboken, N. J.
- Khilar, K. C., and H. C. Fogler (1984), The existence of a critical salt concentration for particle release, *J. Colloid Interface Sci.*, 101(1), 214–224.
- Kjaergaard, C., P. Moldrup, L. W. de Jonge, and O. H. Jacobsen (2004), Colloid mobilization and transport in undisturbed soil columns. II. The role of colloid dispersibility and preferential flow, *Vadose Zone J.*, 3, 424–433.
- Kretschmar, R., K. Barmettler, D. Grolimund, Y. Yan, M. Borkovec, and H. Sticher (1997), Experimental determination of colloid deposition rates and collision efficiencies in natural porous media, *Water Resour. Res.*, 33(5), 1129–1137.
- Laegdsmand, M., K. G. Villholth, M. Ullum, and K. H. Jensen (1999), Processes of colloid mobilization and transport in macroporous soil monoliths, *Geoderma*, 93, 33–59.
- Levin, J. M., J. S. Herman, G. M. Hornberger, and J. E. Saiers (2006), Colloid mobilization from a variably saturated intact soil core, *Vadose Zone J.*, 5, 564–569.
- McCarthy, J. F., and J. M. Zachara (1989), Subsurface transport of contaminants, *Environ. Sci. Technol.*, 23(5), 496–502.
- McKay, L. D., W. E. Sanford, and J. M. Strong (2000), Field-scale migration of colloidal tracers in a fractured shale sapolite, *Ground Water*, 38(1), 139–147.
- Nielsen, D. R., and J. W. Biggar (1962), Miscible displacement. III. Theoretical considerations, *Soil Sci. Soc. Am. Proc.*, 26, 216–221.
- Nielsen, D. R., M. T. van Genuchten, and J. W. Biggar (1986), Water flow and solute transport processes in the unsaturated zone, *Water Resour. Res.*, 22, 89S–108S.
- Rousseau, M. (2003), Particle transport in an unsaturated soil: From experiments in an undisturbed column to the built of a physically-based model, Ph.D. thesis, 242 pp., Inst. Natl. Polytech. de Grenoble, Grenoble, France.
- Rousseau, M., S. Ruy, L. Di Pietro, and R. Angulo-Jaramillo (2004a), Unsaturated hydraulic conductivity of structured soils from a kinematic wave approach, *J. Hydraul. Res.*, 42, 83–91.
- Rousseau, M., L. Di Pietro, R. Angulo-Jaramillo, D. Tessier, and B. Cabibel (2004b), Preferential transport of soil colloidal particles: Physicochemical effects on particle mobilization, *Vadose Zone J.*, 3, 247–261.
- Roy, S. B., and D. A. Dzombak (1996), Colloid release and transport processes in natural and model porous media, *Colloids Surf. A*, 107, 245–262.
- Ryan, J. N., and M. Elimelech (1996), Colloid mobilization and transport in groundwater, *Colloids Surf. A*, 107, 1–56.
- Saiers, J. E., and J. L. Lenhart (2003), Colloid mobilization and transport within unsaturated porous media under transient-flow conditions, *Water Resour. Res.*, 39(1), 1019, doi:10.1029/2002WR001370.
- Schelde, K., P. Moldrup, O. H. Jacobsen, H. de Jonge, L. W. de Jonge, and T. Komatsu (2002), Diffusion-limited mobilization an transport of natural colloids in macroporous soil, *Vadose Zone J.*, 1, 125–136.
- Sposito, G., W. A. Jury, and V. K. Gupta (1986), Fundamental problems in the stochastic convection-dispersion model of solute transport in aquifers and field soils, *Water Resour. Res.*, 22, 77–88.
- Weiss, M., Y. Lüthi, J. Ricka, T. Jörg, and H. Bebie (1998), Colloidal particles at solid-liquid interfaces: Mechanism of desorption kinetics, *J. Colloid Interface Sci.*, 206, 322–331.
- Zhuang, J., Y. Jin, and M. Flury (2004), Comparison of colloids and kaolinite transport in porous media, *Vadose Zone J.*, 3, 395–402.

R. Angulo-Jaramillo, S. Majdalani, and M. Rousseau, LTHE, B.P. 53, F-38041 Grenoble Cedex 9, France. (samer.majdalani@hmg.inpg.fr)

L. Di Pietro and E. Michel, Unité Climat, Sol et Environnement, Institut National de la Recherche Agronomique, Domaine St. Paul, F-84914 Avignon Cedex 9, France.